2014; 18: 257-264

High resolution 3-T MR imaging in the evaluation of the trigeminal nerve course

M. CASSETTA, N. PRANNO, V. POMPA¹, F. BARCHETTI¹, G. POMPA

Department of Oral and Maxillofacial Sciences, School of Dentistry, and ¹Department of Radiological, Oncology and Anatomo-Pathological Sciences; "Sapienza" University of Rome, Rome, Italy

Abstract. – BACKGROUND: The evaluation of the trigeminal course and his anatomical relationships with surrounding structures, is important for the assessment of the injury that may occur in tumors and several orofacial trauma and for avoiding the damage during surgeries.

AIM: The aim of this retrospective study was to assess the use of 3-T MRI in the evaluation of the course of the four segments of the trigeminal nerve: cisternal and Meckels's cave, cavernous sinus, skull base and mandibular extracranial segments.

PATIENTS AND METHODS: 78 patients were studied, for a total of 156 trigeminal nerves examined. T2-weighted 3D Fast imaging employing steady-state acquisition and T1-weighted Fast spoiled gradient recalled echo sequences were used. Two radiologists (reader A and B), independently, evaluated the course of the four segments of the trigeminal nerve according to a qualitative scale. The Intraclass correlation coefficient (ICC) and Pearson correlation coefficient were used to assess the intraobserver and interobserver variability in the nerve course evaluation.

RESULTS: Reader A evaluated 47 trigeminal nerves excellent, 94 good, 12 fair and 3 poor. Reader B rated 43 trigeminal nerves excellent, 92 good, 16 fair and 5 poor. The intraobserver variability was ICC = 0.937 in reader A and ICC = 0.894 in reader B. The interobserver variability was 0.734 ($\rho \le 0.01$).

CONCLUSIONS: High resolution 3-T MRI imaging allows an accurate study of the trigeminal nerve and especially of its mandibular branch. The knowledge of the course and of the anatomic relationships of these nerve bundles with surrounding structures, as well as of the anatomical variants, allow oral and maxillofacial surgical plannings thus reducing the risk of nerve damage.

Key Words:

Magnetic resonance imaging, Trigeminal nerve, Trigeminal nerve injuries, Mandibular nerve, Tomography, X-Ray computed.

Introduction

The trigeminal nerve is the largest cranial nerve and the most widely distributed in the supra-hyoid neck¹. It is a mixed sensory-motor nerve, receiving sensory input from the face and providing motor innervation to the muscles of mastication.

The evaluation of the trigeminal course and his anatomical relationships with surrounding structures is important for the assessment of the injury that may occur in tumors and several orofacial trauma and for avoiding damage during surgeries

A clinical examination using different tests has thus far been the only established method of diagnosing nerve lesions. The using of infrared equipment and magnetoencepahlography are described in some publications to differ between interrupted and intact nerves but these methods, like other available tests, allow nerve lesions to be detected only indirectly^{2,3}.

In patients with mandible fracture accompanied by dysesthesia of the lower lip, panoramic radiographs, and CT show the severe dislocation of the mandible fracture, but it is impossible to know whether the nerve is interrupted, which is very important in designing corrective surgical procedures⁴⁻⁷.

Magnetic resonance imaging (MRI) can provide highly detailed anatomical information with excellent discrimination of the soft tissues, avoiding patient's exposure to X-rays⁸. In the previous studies the limited use of MRI is due to the longer examination time and the lower resolution that this method has in comparison with computed tomography. Indeed, the insufficient spatial resolution 1.5T MRI cannot display small lesion and detail small anatomical structures properly.

Some researchers have demonstrated that the introduction of high resolution 3-T MR and opti-

mized sequences can significantly improve the spatial resolution and the signal-noise ratio (SNR)⁹⁻¹¹.

The aim of this retrospective study was to assess the use of 3 T MR imaging in the evaluation of the course of the trigeminal nerve and especially of its third mandibular branch.

Patients and Methods

Patient Population

The head and neck MRI scans of 78 patients (42 males and 36 females; mean age: 57 years; range: 17 to 71 years) were retrospectively evaluated in the Department of Radiological Science of "Sapienza" University of Rome, Italy.

The study was approved by the local Ethical Committee and conducted in accordance with the Helsinki Declaration of 1975 as revised in 2000.

MR Imaging Acquisition Protocol

All patients underwent an MRI examination performed using a superconducting magnet of 3 Tesla (Discovery MR750, GE Healthcare, Milwaukee, USA) equipped with an 8-channel neurovascular phased-array coil (GE Medical System). The standardized imaging protocol included: axial T1-weighted TSE sequence; axial T2-weighted TSE sequence; axial STIR sequence; axial, coronal and sagittal T1-weighted fat-saturated sequences after gadolinium injection; T2-weighted 3D-Fast imaging employing steady-state acquisition (3D FIESTA) and T1-weighted Fast spoiled gradient recalled echo (fast SPGR) sequences. 3D FIESTA and fast SPGR sequences were used to depict the trigeminal nerve course.

Imaging parameters of 3D FIESTA sequence were as follows: repetition time (TR) = 4.6 ms; echo time (TE) = 2.2 ms; slice thickness = 0.6 mm; field of view (FOV) = 20×20 cm; number of excitations (NEX) = 1; matrix = 512×512 .

Imaging parameters of fast SPGR sequence were as follows: repetition time (TR) = 8 ms; echo time (TE) = 3 ms; slice thickness = 0.6 mm; field of view (FOV) = 15×21 cm; number of excitations (NEX) = 2; matrix = 512×512 .

Axial acquisition were obtained for both sequences.

MRI Post-Processing and Image Interpretation

Two experts in oral radiology (reader A with 25 years of experience and reader B with 5 years of experience) evaluated, independently, the images

of the trigeminal nerve. The images were evaluated on an off-line dedicated workstation (AW Volume-Share2, GE Healthcare, Milwaukee, USA). Optimal planes, including the course of the inferior alveolar nerve (IAN), were determined by means of multiplanar reformation (MPR) using the imager's standard reformation software (Figure 1).

The radiologists, to simplify the trigeminal nerve evaluation, divided the anatomical course into 4 segments: cisternal and Meckels's cave, cavernous sinus, skull base and mandibular extracranial segments. The course of each segment was rating as described below:

Unclear course: 1; Probable recognition of the course: 2; Definite recognition of the course: 3.

The presence of motion artifacts was rated in each segment as follows:

Severe artifacts: 1; Mild artifacts: 2; None: 3.

The sum of the scores of each component determines, according to the following conversion scale, the accuracy degree to depict the full trigeminal nerve course:

Score from 24 to 20: excellent; Score from 19 to 14: good Score from 13 to 8: fair; Score < 8: poor.

After 2 months, the two specialists reassessed the course of the trigeminal segments in order to calculate the intraobserver variability.

Statistical Analysis

Data were evaluated using a statistical analysis software (SPSS®, Statistical Package for Social Science, IBM Corporation, Armonk, NY, USA).

Qualitative data of accuracy degree in the depiction of the trigeminal nerve course (excellent, good, fair and poor) were described with frequency distribution. To evaluate reproducibility, the two experts repeated the evaluation of the trigeminal nerves on two occasions at intervals of 2 months. Intraclass correlation coefficient (ICC) were used to evaluate intraobserver variability. Pearson correlation coefficient was used to evaluate the interobserver variability. The significance was set at $p \le 0.01$.

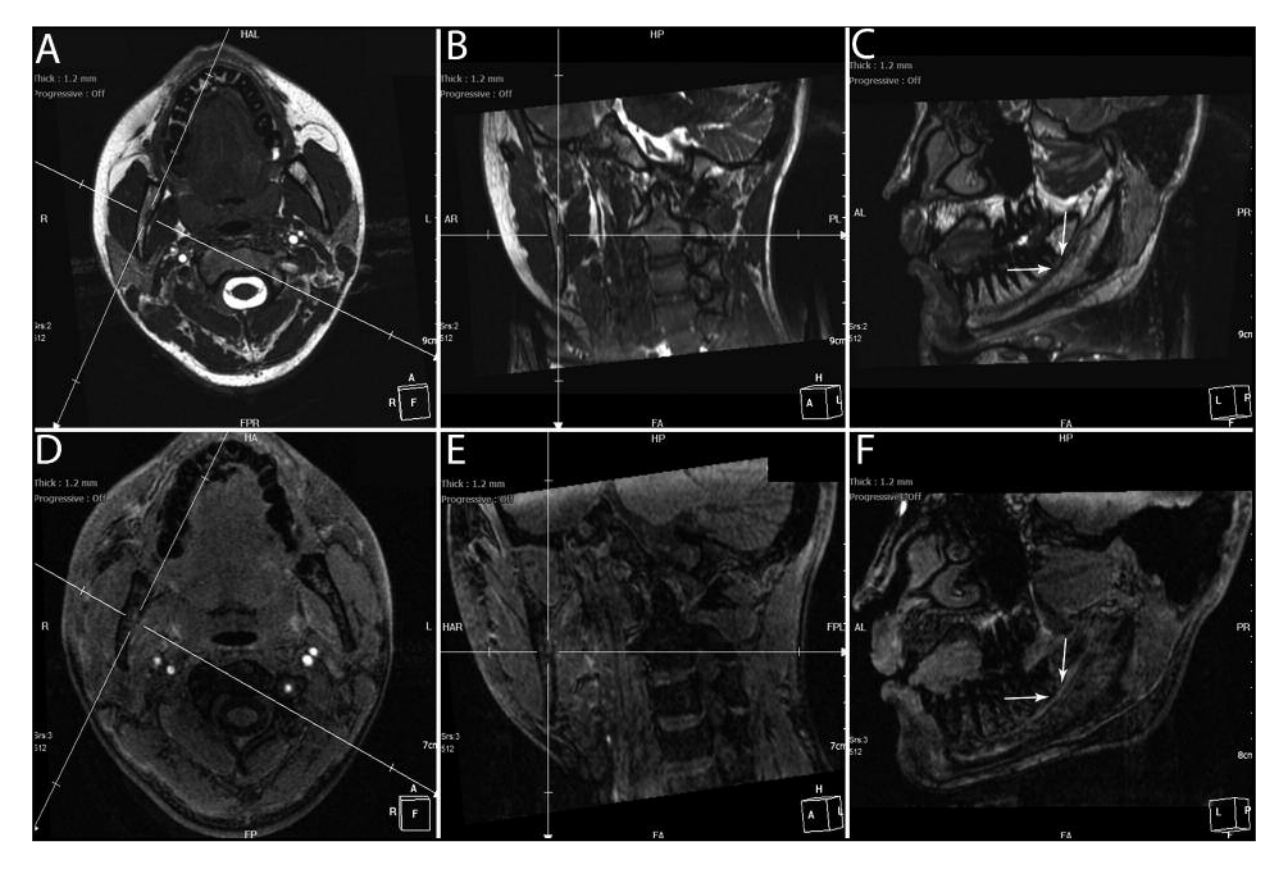


Figure 1. 3D FIESTA **(A-C)** and 3D SPGR **(D-F)** images showing the procedure needed to obtain an optimal plane to display the IAN. In multiplanar reformation (MPR) technique the reference axis were centered in the proper axial images at the level of the mandibular third molar with an axis oriented parallel and the other perpendicular to alveolar bone in order to achieve a parasagittal plane to correctly depict the course of the IAN. **C, F,** The relationship with the IAN and third molar roots is well displayed (white arrows).

Results

The frequency distribution of accuracy degree in the depiction of the trigeminal nerve segments course, according to reader A and reader B, is summarized in Table I.

The cisternal segment was identified at the ventrolateral midpons where the trigeminal nerve emerges as two separate roots. The larger sensory root was located laterally and the smaller motor root medially (Figure 2A) and penetrated into Meckel's cave containing the gasserion ganglion. The sensory root entered the ganglion and divid-

Table I. Qualitative assessment of full trigeminal course.

Qualitative assessment	Reader A	Reader B
Excellent	47 = 28.8%	43 = 27.6%
Good	94 = 61.6%	92 = 59.1%
Fair	12 = 7.7%	16 = 10.2%
Poor	3 = 1.9%	5 = 3.1%

ed into 3 branches: ophthalmic, maxillary and mandibular (Figure 2B). The motor root went through under the ganglion, turned inferiorly to exit the skull base together with the mandibular division of the sensory root¹².

In the cavernous segment the ophthalmic and maxillary divisions continued within the lateral wall of the cavernous sinus (Figure 2C), below the cavernous part of internal carotid artery¹².

In the skull base segment the ophthalmic division leaved the anterior cavernous sinus and exited the intracranial compartment through the superior orbital fissure (Figure 2D), the maxillary division exited the central skull base through foramen rotundum and entered the pterygopalatine fossa¹³ (Figures 2E, F) and the mandibular division, the largest of the three, exited the skull base through foramen ovale, entering the nasopharyngeal masticator space (Figures 3A, B).

The mandibular peripheral segment gave off 4 sensory branches: buccal, auriculotemporal, lingual and inferior alveolar nerve (IAN). The divi-

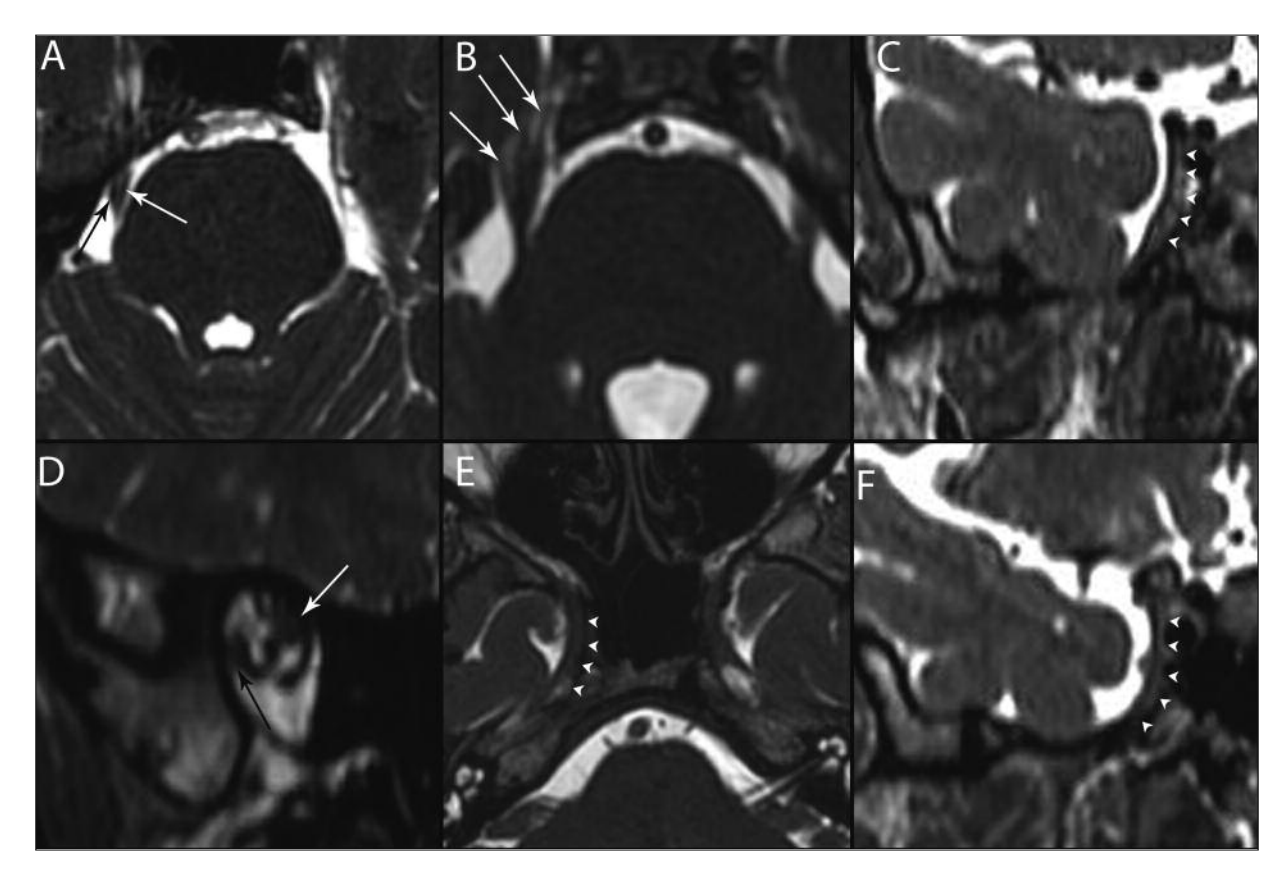


Figure 2. *A,* Axial 3D FIESTA image through the ponto-mesencephalic junction shows the cisternal segment of the trigeminal nerve travelling through the lateral aspect of the pre-pontine cistern, with the larger sensory root located laterally (*black arrow*) and the smaller motor root placed medially (*white arrow*). *B,* Axial 3D FIESTA image through the high pons demonstrates the nerve entering the medial cranial fossa and penetrating a dural lined sinus filled with cerebro-spinal-fluid, Meckel's cave, containing the gasserion ganglion. The sensory root enters the ganglion and divides into 3 branches: ophthalmic, maxillary and mandibular (*white arrows*). *C,* Coronal 3D FIESTA image shows the ophthalmic and maxillary divisions of the trigeminal nerve within the lateral wall of the cavernous sinus (*white arrowheads*), below the cavernous part of internal carotid artery. *D,* Coronal 3D FIESTA image shows the ophthalmic division (*black arrow*) leaving the anterior cavernous sinus and the intracranial compartment through the superior orbital fissure (white arrow: oculomotor nerve). *E, F,* Axial and coronal 3D FIESTA images display the maxillary division of the trigeminal nerve travelling from the inferior cavernous sinus to the pterygopalatine fossa through the foramen rotundum (*white arrowheads*).

sion of mandibular branch in IAN and lingual nerve was found 8 mm beneath the foramen ovale (Figure 3C).

The IAN entered the mandibular canal through the mandibular foramen (Figure 4A) at the lingual surface of the mandibular ramus and travelled along the body of the mandible (Figures 1C, F, 4B). It divided at the first and second premolars teeth into terminal incisive and mental branches. The mental nerve emerged at the mental foramen and innervated the skin of the chin and the mucous membrane of the lower lip (Figure 4C). The incisive nerve ran from the mental nerve usually to the region of the ipsilateral incisor teeth (Figure 4D)¹¹. The lingual nerve lied at first beneath the lateral pterygoid muscle me-

dial to and in front of IAN. The nerve then passed between the medial pterygoid muscle and the ramus of the mandible, and crossed obliquely to the side of the tongue over the costrictor pharyngis superior and styloglossus. From there, it passed between the mylohyoid muscle and the mucous membrane of the floor of the mouth along the side of the tongue (Figure 4B).

Both readers were not able to identify the buccal and auriculotemporal branches in all patient.

The intraobserver variability in the evaluation of the trigeminal nerve course was ICC = 0.937 in reader A and ICC = 0.894 in reader B.

The interobserver variability in the assessment of the trigeminal segments (Pearson correlation coefficient) was 0.734 ($p \le 0.01$).

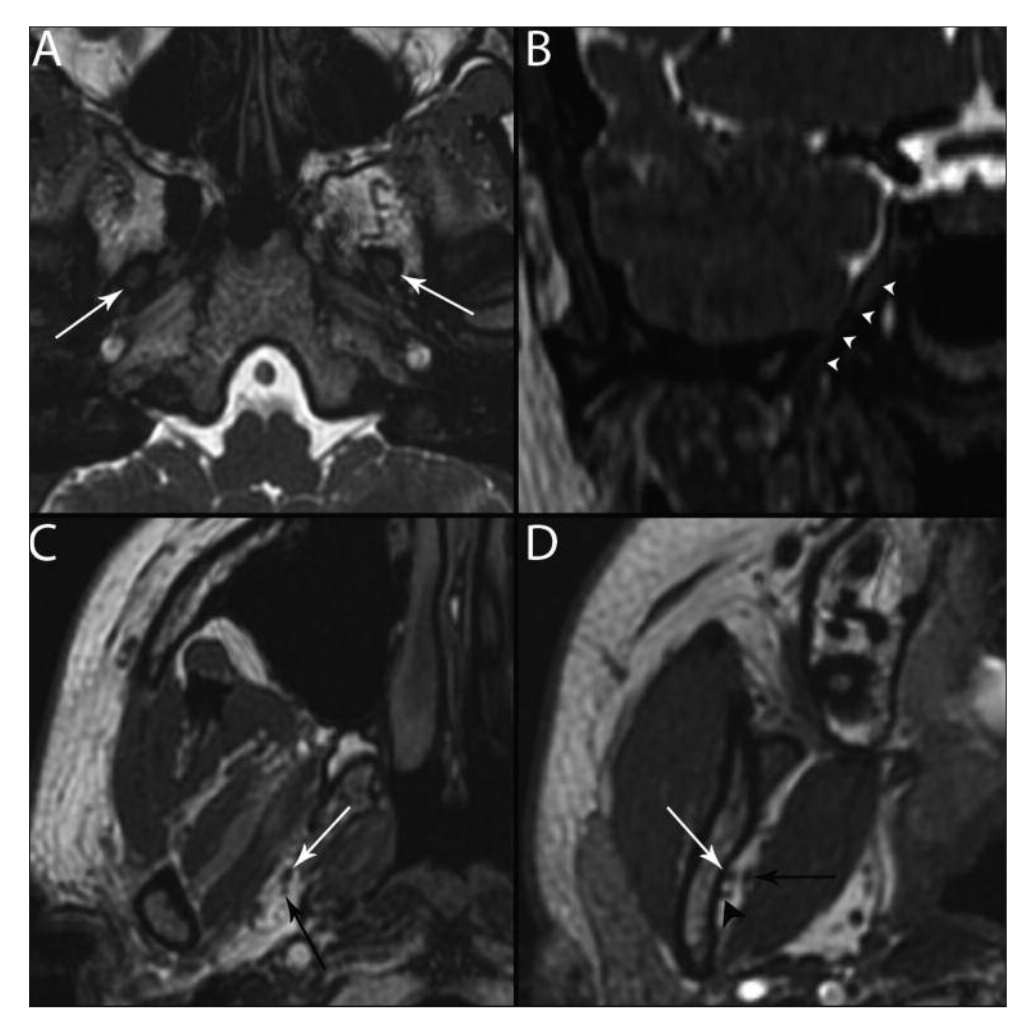


Figure 3. *A, B,* Axial and coronal 3D FIESTA images show the mandibular division leaving the skull base through foramen ovale and entering the nasopharyngeal masticator space. *C,* Axial 3D FIESTA image depicting the division of the mandibular branch in inferior alveolar nerve (*black arrow*) and lingual nerve (*white arrow*) at about 8 mm beneath the foramen ovale. *D,* Axial 3D FIESTA image showing the IAN (*white arrow*), mylohyoid nerve (*black arrowhead*) braching from the IAN and the lingual nerve (*black arrow*) runnig medially to the IAN.

Discussion

To know the course of the cranial nerves before the surgical planning is of primary importance to avoid the risk of nerve bundles injury.

In the previous studies, MRI with conventional field strength did not allow the evaluation of the course of the cranial nerves (although it has always been considered the gold standard for the study of the nervous system), because the conventional 1.5 Tesla magnet is not enable to reach high spatial resolution so as to acquire images suitable for the study of the cranial nerves which have small diameter and tortuous course. Another drawback is a high incidence of motion artifacts related to the high interval of time necessary for

the acquisition of the images. Recently, the introduction into clinical practice of high-field strength MR systems (3.0 Tesla) and the use of fast sequences such as 3D FIESTA, has brought clear advantages. The main advantage of a 3.0 Tesla magnet is the increasing in the signal-tonoise ratio, which leads to a gain of the spatial resolution with improving the quality of images ¹⁵. 3D FIESTA allows the acquisition of images with a submillimetric section thicknesses in a very short time, with a consequent reduction of the motion artifacts allowing the study of smaller structures such as nerve bundles.

An 3D FIESTA sequence is any gradient-echo sequence in which a nonzero steady state develops between pulse repetitions for both the longi-

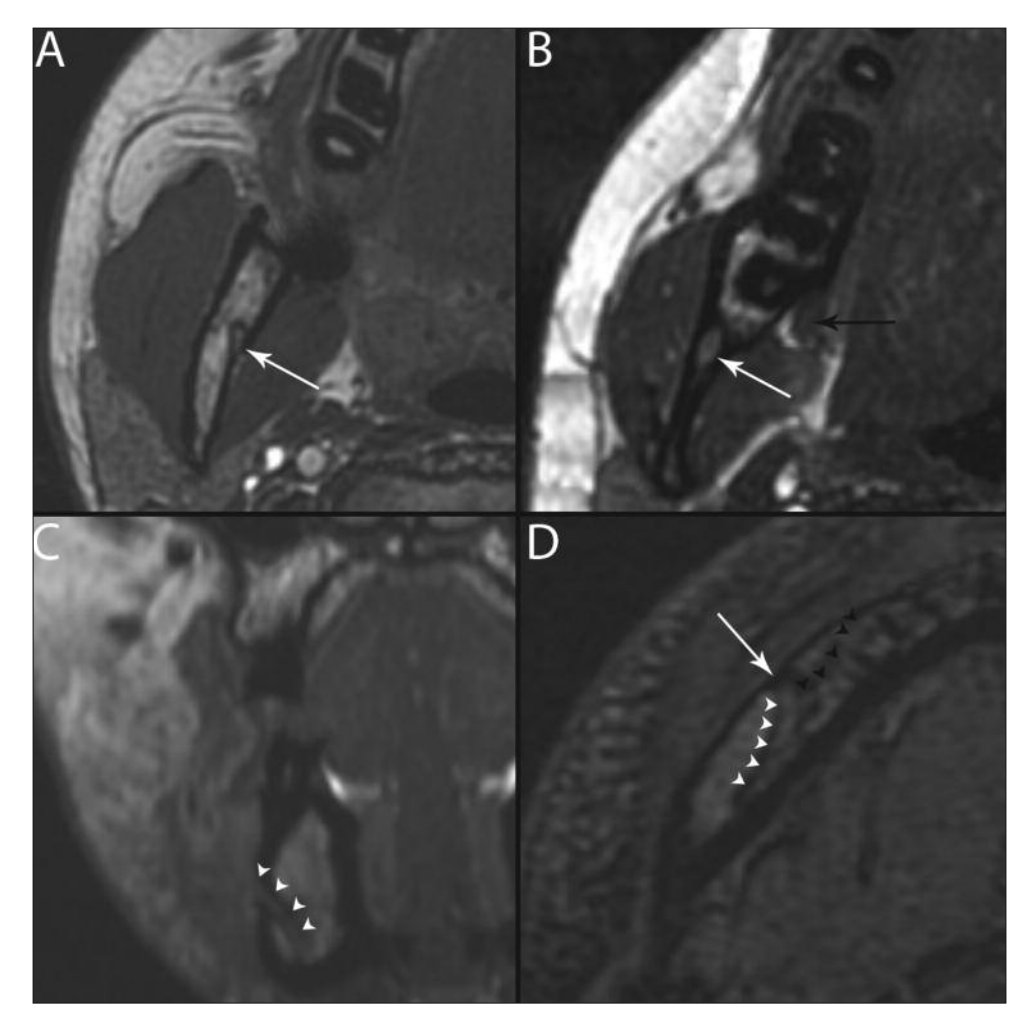


Figure 4. A, Axial 3D FIESTA image shows the IAN (*white arrow*) entering the mandibular canal through the mandibular foramen at the lingual surface of the mandibular ramus. **B,** Axial 3D FIESTA image displays the IAN (*white arrow*) travelling along the body of the mandible and the lingual nerve (*black arrow*) running between the mylohyoid muscle and the mucous membrane of the floor of the mouth along the side of the tongue. **C,** Coronal 3D FIESTA image shows the mental nerve (*white arrowheads*) emerging at the mental foramen and entering into the soft-tissues of the chin and the lower lip. **D,** Axial fast SP-GR image shows the IAN (*white arrowheads*) travelling along the body of the mandible, the mental foramen (*white arrow*) and the incisive nerve (*black arrowheads*) running from the mental nerve to the region of the ipsilateral incisor teeth.

tudinal and transverse relaxation values of the interrogated tissues. A small flip angle and short relaxation time are required for this to occur. The clinical utility of an 3D FIESTA sequence lies in its ability to generate a strong signal in tissues that have a high T2/T1 ratio, such as cerebrospinal fluid (CSF) and fat¹⁶.

The use of 3.0 Tesla MR imaging with 3D FIESTA sequence allows to reach a higher spatial resolution and a decrease of motion artifacts, with a consequent clearer depiction of tiny cranial nerve bundles, showed as low signal intensity structures.

The main disadvantage of 3D FIESTA imaging is a reduced contrast resolution between hard

and soft tissues that does not allow the visualization of peripheral branches inside mandibular bone. This drawback can be overcome by the use of T1-weighted fast spoiled gradient recalled echo (fast SPGR). Fast SPGR is a 3D fast fat saturated T1-weighted sequence which provides a high contrast between nerve bundles, displayed as a high signal intensity structure, and bone tissue, depicted as a very low signal intensity structure (Figures 1F, D).

This study has been focused on the trigeminal nerve and especially on the mandibular branch. Indeed the knowledge of the IAN and the lingual nerve course (the two main branches of the mandibular nerve) is of a great importance in oral and maxillofacial surgery, because they are at risk of injury that may occur in tumors, trauma and several orofacial surgical procedures such as extraction of the mandibular third molar, orthognathic surgery of the mandible 17-21, root canal treatment, block anesthesia and dental implant surgery 22. The damage of these nerve trunks may result in neurosensory impairment ranging from the complete anesthesia to the more common partial loss of sensitivity.

In the past, during orofacial surgeries, the knowledge of anatomy of the lingual and inferior alveolar nerves was based only on data derived from surveys carried out on basic studies on cadaveric mandibles²³. For this reason any information about anatomical variations was not provided therefore the risk of the damage of the nerve bundles was always present. Detailed MRI anatomical studies, however, would provide the surgeon with the exact knowledge of the course of these nerves and the relationships with local anatomical landmarks and any existing variants allowing surgical planning to be designed safely and thus avoiding possible nerve injuries.

The high intraobserver ICCs and high interobserver Pearson correlation coefficient found in this study indicate high degree of reliability and a high level of reproducibility in the evaluation of trigeminal nerve course.

Our findings suggest that the MRI study of the trigeminal nerve course could get into the routine surgical planning with all the important advantages that can result in clinical practice; for instance the distance of the IAN to the apices of the teeth or the alveolar ridge can be measured and this can decrease the possibility of nerve injury in dental implant and extraction of the third molars (Figures 1C, F).

Conclusions

The use of 3.0 T MRI with 3D FIESTA and fast SPGR sequences allowed the study of the course of the trigeminal nerve and its branches. The knowledge of the course and of the anatomic relationships of these nerve bundles with surrounding structures, as well as of the anatomical variants, allow oral and maxillofacial surgical plannings thus reducing the risk of nerve damage. The reduced appearance of this complication provides advantages both for the patient, in terms of safety, and for the physician, in terms of medico-legal consequences.

Conflict of Interest

The Authors declare that there are no conflicts of interest.

References

- WILLIAMS LS, SCHMALFUSS IM, SISTROM CL, INOUE T, TANAKA R, SEOANE ER, MANCUSO AA. MR imaging of the trigeminal ganglion, nerve, and the perineural vascular plexus: normal appearance and variants with correlation to cadaver specimens. AJNR Am J Neuroradiol 2003; 24: 1317-1323.
- McDonald AR, Roberts TP, Rowley HA, Pogrel MA. Noninvasive somatosensory monitoring of the injured inferior alveolar nerve using magnetic source imaging. J Oral Maxillofac Surg 1996; 54: 1068-1072.
- GRATT BM, SHETTY V, SAIAR M, SICKLES EA. Electronic thermography for the assessment of the inferior alveolar nerve deficit. Oral Surg Oral Med Oral Pathol Oral Radiol Endod 1995; 80: 153-160.
- 4) TANTANAPORNKUL W, OKOUCHI K, FUJIWARA Y, YA-MASHIRO M, MARUOKA Y, OHBAYASHI N et al. A comparative study of cone-beam computed tomography and conventional panoramic radiography in assessing the topographic relationship between the mandibular canal and impacted third molars. Oral Surg Oral Med Oral Pathol Oral Radiol Endod 2007; 103: 253-259.
- Susarla SM, Dodson TB. Preoperative computed tomography imaging in the management of impacted mandibular third molars. J Oral Maxillofac Surg 2007; 65: 83-88.
- CASSETTA M, STEFANELLI LV, DI CARLO S, POMPA G, BAR-BATO E. The accuracy of CBCT in measuring jaws bone density. Eur Rev Med Pharmacol Sci 2012; 16: 1425-1429.
- CASSETTA M, STEFANELLI LV, GIANSANTI M, DI MAMBRO A, CALASSO S. Accuracy of a computer-aided implant surgical technique. Int J Periodontics Restorative Dent 2013; 33: 317-325.
- MAZZA D, MARINI M, IMPARA L, CASSETTA M, SCARPATO P, BARCHETTI F, DI PAOLO C. Anatomic examination of the upper head of the lateral pterygoid muscle using magnetic resonance imaging and clinical data. J Craniofac Surg 2009; 20: 1508-1511.
- DENG W, CHEN SL, ZHANG ZW, HUANG DY, ZHANG X, LI X. High-resolution magnetic resonance imaging of the inferior alveolar nerve using 3-dimensional magnetization-prepared rapid gradient-echo sequence at 3.0T. J Oral Maxillofac Surg 2008; 66: 2621-2626.
- 10) CASSETTA M, DI CARLO S, PRANNO N, STAGNITTI A, POMPA V, POMPA G. The use of high resolution magnetic resonance on 3.0-T system in the diagnosis and surgical planning of intraosseous lesions of the jaws: preliminary results of a retrospective study. Eur Rev Med Pharmacol Sci 2012; 16: 2021-2028.
- 11) Go JL, KIM PE, ZEE CS. The trigeminal nerve. Semin Ultrasound, CT, MR 2001; 22: 502-520.

- Borges A, Casselman J. Imaging the cranial nerves part I: methodology, infectious and inflammatory, traumatic and congenital lesions. Eur Radiol 2007; 175: 2112-225.
- BORGES A, CASSELMAN J. Imaging the cranial nerves part II: primary and secondary neoplastic conditions and neurovascular conflicts. Eur Radiol 2007; 17: 2332-2344.
- BORGES A. Trigeminal nevralgia and facial nerve paralysis. Eur Radiol 2005; 15: 511-533.
- 15) FISCHBACH F, MÜLLER M, BRUHN H. Magnetic resonance imaging of the cranial nerves in the posterior fossa: a comparative study of T2-weighted spin-echo sequences at 1.5 and 3.0 tesla. Acta Radiol 2008; 49: 358-363.
- CHAVHAN GB, BABYN PS, JANKHARIA BG, CHENG HL, SHROFF MM. Steady-state MR imaging sequences: physics, classification, and clinical applications. RadioGraphics 2008; 28: 1147-1160.
- 17) CASSETTA M, DI CARLO S, GIANSANTI M, POMPA V, POM-PA G, BARBATO E. The impact of osteotomy technique for corticotomy-assisted orthodontic treatment (CAOT) on oral health-related quality of life. Eur Rev Med Pharmacol Sci 2012; 16: 1735-1740.
- 18) CASSETTA M, DI MAMBRO A, GIANSANTI M, STEFANELLI LV, BARBATO E. Is it possible to improve the accuracy of implants inserted with a stereolithographic surgical guide by reducing the tolerance between

- mechanical components? Int J Oral Maxillofac Surg 2013; 42: 887-890.
- 19) CASSETTA M, POMPA G, DI CARLO S, PICCOLI L, PACIFICI A, PACIFICI L. The influence of smoking and surgical technique on the accuracy of mucosa-supported stereolithographic surgical guide in complete edentulous upper jaws. Eur Rev Med Pharmacol Sci 2012; 16: 1546-1553.
- 20) CASSETTA M, RICCI L, IEZZI G, DELL'AQUILA D, PIATTELLI A, PERROTTI V. Resonance frequency analysis of implants inserted with a simultaneous grafting procedure: a 5-year follow-up study in man. Int J Periodontics Restorative Dent 2012; 32: 581-589.
- 21) TATULLO M, MARRELLI M, CASSETTA M, PACIFICI A, STE-FANELLI LV, SCACCO S, DIPALMA G, PACIFICI L, INCHINGO-LO F. Platelet Rich Fibrin (P.R.F.) in reconstructive surgery of atrophied maxillary bones: clinical and histological evaluations. Int J Med Sci 2012; 9: 872-880.
- 22) TERUMITSU M, SEO K, MATSUZAWA H, YAMAZAKI M, KWEE IL, NAKADA T. Morphologic evaluation of the inferior alveolar nerve in patients with sensory disorders by high-resolution 3D volume rendering magnetic resonance neurography on a 3.0-T system. Oral Surg Oral Med Oral Pathol Oral Radiol Endod 2011; 111: 95-102.
- IKEDA K, HO KC, NOWICKI BH, HAUGHTON VM. Multiplanar MR and anatomic study of the mandibular canal. AJNR Am J Neuroradiol 1996; 17: 579-584.